Sensors and Actuators Reports 5 (2023) 100153

Contents lists available at ScienceDirect

Sensors and Actuators Reports

journal homepage: www.sciencedirect.com/journal/sensors-and-actuators-reports

Molecularly imprinted polymer (MIP) based electrochemical sensors and their recent advances in health applications

Lue Wang [a,b], Wei Zhang [a,*]

[a] Department of Chemical Engineering, Swansea University, Swansea SA1 8EN, UK
[b] School of Pharmaceutical Sciences, Tsinghua University, 100084, Beijing, China

ARTICLE INFO

Keywords:
Molecularly imprinted polymer (MIP)
Electrochemical
Sensor
Health application
Clinical

ABSTRACT

Molecularly imprinted polymer (MIP)-based electrochemical sensors have received growing attention over past decades owing to its robust nature, simple electrochemical control for template removal and cavity regeneration, and go-as-you-please cavity designs into various geometries specific to target analytes. The strength of MIP scheme, in combination with the advantages of electrochemical sensing techniques such as operation simplicity, rapid response, and high sensitivity, provide a synergistic effort to form a highly effective sensing platform suitable for an extremely wide range of interest. In this Review, the introduction of MIP and the comparison between electrochemical sensing methods and other detection strategies are briefly discussed. Then, a broad range of analytes determined using MIP-based electrochemical sensors are listed and critically reviewed, mainly focusing on the applied electrochemical technique, presented linear range along with limit of detection (LOD), biological fluid used in real testing, and pretreatment for real sample. Other sensor performances like selectivity towards analyte, signal repeatability, sensor-to-sensor reproducibility, and stability, are carefully compared with other reported papers. MIP sensors fabricated via the nanoMIP technology, and the ones integrated with portable analyzers, are given in more details as good results are always observed in such instances. Finally, a conclusion regarding recent advances on MIP-based electrochemical sensors is presented, followed by current issues and future development depicted at the last section of the Review.

Abbreviations

AAs	amino acids
aGO/CB	acryloylated-graphene oxide/carbon black
ASCVDs	atherosclerotic cardiovascular diseases
AuNPs	gold nanoparticles
Au-TFME	gold-thin-film metal electrode
BCAAs	branched-chain amino acids
CD56	neural cell adhesion molecule
CEA	carcinoembryonic antigen
CHO	cholesterol
COC	cyclic olefin copolymer
COVID-19	coronavirus disease 2019
cTnI	cardiac troponin I
DA	dopamine
DM	diabetes mellitus
DMFC	direct methanol fuel cell
DPV	differential pulse voltammetry
DPASV	differential pulse anodic stripping voltammetry
DPSV	differential pulse stripping voltammetry
ECL	electrochemiluminescence
EIS	electrochemical impedance spectroscopy
EP	epinephrine
EtOH	ethanol
GCE	glassy carbon electrode
GO	graphene oxide
HSA	human serum albumin
IDA	interdigitated array
IF	imprinting factor
IL	ionic liquid
Ile	isoleucine
LEG	laser-engraved graphene
Leu	leucine
LOD	limit of detection
LSV	linear sweep voltammetry
Mb	myoglobin
MES	2-morpholinoethanesulfonic acid
MIP	molecularly imprinted polymer

* Corresponding author.

https://doi.org/10.1016/j.snr.2023.100153
Received 28 February 2023; Received in revised form 10 April 2023; Accepted 17 April 2023
Available online 24 April 2023

MIPMs	molecularly imprinted polymeric micelles
NCAM1	neural cell adhesion molecule 1
ncovS1	SARS-CoV-2 spike protein subunit S1
NIP	non-imprinted polymer
NSE	neuron specific enolase
PBS	phosphate buffered saline
PEC	photoelectrochemical
RAR	redox-active nano-reporters
RSD	relative standard deviation
SAC	sarcosine
SARS-CoV-2	severe acute respiratory syndrome coronavirus 2
SARS-CoV-2-RBD	SARS-CoV-2-receptor binding domain
SCLC	small cell lung cancer
SPE	screen-printed electrode
SPS	sample preservation solution
SWV	square wave voltammetry
Trp	Tryptophan
Tyr	tyrosine
Val	valine
WADA	World Anti-Doping Agency

1. Introduction

Scientific research on sensors is of a hot spot in recent decades. The word of sensor can be generally interpreted as a functionalized platform that provides signal transduction from unreadable physical or chemical events occurring at a specific interface to understandable responses. Sensors with a layer of polymeric molecule-suited cavities, as so-called molecularly imprinted polymer (MIP) sensors, appeal a great deal of attention owing to the unique capability of analyte-recognition. A large variety of methods to analyte determination have been implemented in combination with MIP sensors, including fluorescence [1], surface enhanced Raman scattering [2], surface plasmon resonance [3,4], and electrochemical schemes [5,6]. Among them, electrochemical sensing has been increasingly reported as it is regarded as a more effective strategy for detection of various molecules in biofluids over other techniques [7,8,9,10,11], attributed to natures of simple manipulation, rapid response, cost-effectiveness, and portability [12,13,14,15,16,17].

Electrochemical sensors with MIP functional component exhibit excellent detection capability towards a wide range of target analytes, including biomarkers, endocrine hormones, and body-related chemicals, proteins, and drugs [18,19]. Nonetheless, most of studies elaborate great effort on the modification of electrodes by involving less-reported substances or other unique materials as research novelties, while present less evaluation on the sensor maturity such as the applicability in real samples and integration with portable analyzers. Research-scaled testing is not a destination but is a starting point of the avenue to clinical use and product customization. The situation in actual sensing environment is more complicated than the standard buffer due to the presence of non-specific substances, which often leads to an insensitive monitoring. Hence, functional components with extraordinary durability and analyte specificity are in urgent need to solve this issue. On the other hand, great challenges may also appear in the process of product transformation from laboratory-scaled ensemble to industrial scale-up, including device miniaturization, long-term storage for transportation, and affordability in markets.

This Review mainly focuses on the sensing performances of recently reported MIP-based electrochemical sensors instead of the up-stream electrode surface modification. Studies in aspect of practical use are systematically reviewed and critically compared especially for the ones that have been successfully achieved in real biofluids or clinical circumstances. Approaches in relation to improving sensitivity of MIP-based sensors and the sensors coupled with smart analyzers to form an advanced sensing system, are discussed as a highlight. This review provides an insight understanding of sensing properties and practicability regarding previously reported MIP-based electrochemical sensors, along with a critical discussion on current issues and the tendency of future development, offering a comprehensive and useful guideline for scientific groups or industries to create more intelligent MIP-based electrochemical sensors.

2. Various analytes determined using MIP-based electrochemical sensors

Electrochemical sensors with the functional component of MIP exhibit powerful detection capability towards a wide range of analytes, including biomarkers, body-produced chemicals, and hormones. Comparison data regarding electrochemical techniques employed, range of detection, LOD, real samples tested, and necessary pretreatments, is clearly listed in the following Tables 1 and 2. Further sensing performances, like device sensitivity, analyte selectivity, signal reversibility, electrode fabrication reproducibility, and storability, are well compared at each part of discussion.

2.1. Biomarkers detected using MIP-based electrochemical sensors

Sarcosine (SAR) is a crucial biomarker for effective diagnosis of prostate cancer [31]. Sensitive detection of SAR in biological fluids at trace amount becomes in higher demand as the number of patients suffered from prostate cancer are still growing in recent years. An electrochemical sensor modified with imprinted polymeric nanobeads for SAR detection in urine was reported by Sheydaei et al. [20], and the sensor presented excellent selectivity towards SAR in the presence of other 8 organic interferents due to the good affinity nature of MIP. Moreover, desirable reproducibility obtained from 3 replicates with relative standard deviation (RSD) of 4.6% and repeatability yielded by 3 different sensors with RSD of 2.7%, also confirmed the well sensing behaviors of the sensor. In real sample testing, the proposed sensor was allowed to test the urine samples collected from a healthy man and a 70-year-old patient and spiked with SAR in different concentrations. Recoveries of 97.4% ~ 103.8% with RSD less than 4% showed the sensor had a strong applicability in real biological environment [20]. Sun et al. [21], developed a photoelectrochemical cathodic MIP sensor for sensitive determination of SAR (Fig. 1a). An improved photocurrent of the cathode was achieved due to the self-powered photoanode / photocathode construction, resulting in a wider dynamic range of 0.89 ~ 890.93 ng/mL and a lower LOD of 16.93 pg/mL, compared with the data presented by Sheydaei et al. The change of photocurrent in relation to SAR was recorded as 5 to 10 times higher than those of other 5 interferents, indicating a good selectivity of the PEC-MIP sensor towards the target analyte. Good signal reproducibility was demonstrated by testing SAR with identical concentration on 6 electrodes, and RSD of 5% is obtained. Constant photocurrent was observed after ten cycles of light-dark reaction, proving a nice stability used for sensing applications. The PEC-MIP sensor had applicability to detect SAR in real human serum samples with recoveries of 97.7% ~ 103.2% but had no corresponding RSD [13].

The level of neuron-specific enolase (NSE) in human body fluids has a close association with neuronal damage and small cell lung cancer (SCLC) [32,33]. A NSE level with less than 20 ng/mL is usually observed in serum or cerebrospinal fluid collected from a healthy individual, while specimens from patients are usually detected beyond 100 ng/mL [34,35]. Prizada et al. [22], developed a gold nanoparticle-decorated electrochemical sensor imprinted with two types of epitope-adapted cavities for determination of NSE (Fig. 1b). The hybrid-MIP sensor presented an outstanding sensitivity towards the target in comparison to other reported MIP-sensors of which epitopes modified with single class of amino acid [36,37,38]. An imprinting factor (IF) of 4.2 represented acceptable selectivity of the sensor although it was not very high enough compared with that of the NIPs. The current signal of SWV was observed in almost 35% suppression compared with that after the template removal when the sensor was loaded with half diluted human serum.

Table 1
MIP-based electrochemical sensors used for determination of biomarkers.

Biomarker	Electrochemical Technique	Dynamic Range (ng/mL)	LOD (pg/mL)	Real Body Fluid	Pretreatment for Real Sample	Ref.
SAC	DPV	445.47 ~ 9.8×10^4	3.38×10^4	Urine	Diluted (1:50) with phosphoric acid (pH = 1.0)	[20]
SAC	PEC	0.89 ~ 890.93	16.93	Human serum	Diluted (1:100) with PBS	[21]
NSE	SWV	0.025 ~ 4	25	Human serum	Half diluted with PBS (pH 7.4)	[22]
NSE	DPV	0.01 ~ 1	2.6	Human serum	Diluted (1:100) with PBS (0.01 M, pH 7.4)	[23]
CD56	DPV	0.001 ~ 1	0.47	Human serum	Diluted (1:1000) and filtered through a cellulose membrane	[24]
CEA	Power-current Density	0.1 ~ 10^5	80	Human serum (Cormay® serum)	Diluted with MES buffer (10 mM, pH 6.0)	[25]
CEA	DPV	1 ~ 500	320	Human serum	——	[26]
SARS-CoV-2-RBD	EIS	0.002 ~ 0.04	0.7	Saliva	Diluted (1:1) with PBS (0.2 M, pH 7.4)	[27]
ncovS1	SWV	2.05×10^{-3} ~ 0.015	1.15	Nasopharyngeal swab specimens from patients	Diluted with a mixture (SPS: PBS 1:99)	[28]
cTnI (NanoMIP)	SWV	0.01 ~ 1000	3.2	Human serum	Diluted (1:10) with PBS (0.1 M, pH 7.4)	[29]
cTnI and Mb	ECL	cTnI: 0.05 ~ 10^4 Mb: 0.05 ~ 10^4	18.4 49.2	Serum	Diluted	[30]

Table 2
MIP-based electrochemical sensors used for determination of body-produced chemicals and hormones.

Body-produced chemical and hormones	Electrochemical Technique	Dynamic Range (ng/mL)	LOD (pg/mL)	Real Body Fluid	Pretreatment for Real Sample	Ref.
Glucose	SWV	0.225 ~ 57.65	225	Human serum	Diluted (1:100) with PBS and Undiluted	[49]
Glucose	DPV	500 ~ 5×10^4	5.9×10^5	Saliva	Heated at 100 °C for 30 min, and centrifuged at 1,500 rpm for 15 min	[50]
Glucose	DPSV	3.6×10^4 ~ 1.44×10^6	9×10^6	Simulative serum	1 mM glucose, 0.08 mM ascorbic acid and 0.04 mM uric acid in an actual 20% serum sample	[51]
CHO	DPV	3.87×10^{-5} ~ 0.387	0.013	——	——	[52]
CHO	DPV	3.87×10^{-10} ~ 3.87×10^{-5}	1.3×10^{-7}	Human serum	Diluted (1:10) with perchloric acid, centrifuged, and further diluted (1:10) with ethanol	[53]
DA (NanoMIP)	DPV	7.659×10^{-3} ~ 765.9	1.53	Human serum and urine	Diluted (1:100) with PBS (pH 6.5)	[54]
DA and EP	DPASV	DA: 0.116 ~ 6.231 EP: 0.074 ~ 1.832	26 17	Blood serum and urine	Blood serum: diluted 2-fold Urine: diluted 187.6-fold	[55]
Insulin (NanoMIP)	DPV	0.287 ~ 11.47	0.149	Human plasma	Diluted (1:10) with PBS (10 mM, pH 7.2), agitated for 3 min, centrifuged for 3 min at 3,500 rpm, and the supernatant filtered using a syringe containing a microfiltration membrane	[56]
Testosterone	EIS	2.88×10^{-7} ~ 288.42	1.15×10^{-4}	Human serum	Interfering proteins removed by precipitation with trichloroacetic acid (10%, w/v), centrifuged for 15 min, and diluted (1:10) with PBS (pH 7.0)	[57]
Testosterone	EIS	0.144 ~ 5.76	144	Human urine and saliva	Filtered and diluted with EtOH	[58]

Also, weakened binding affinity of the sensor was confirmed in the serum environment, which was not as good as the one tested in the standard buffer. Such results were probably attributed to the complexity of constituents in human serum that might contain various proteinaceous substance non-specifically bound to the imprinted cavities [22]. Another sensing platform for sensitive detection of NSE was prepared by Wang et al. [23], where the electrode surface was modified with gold nanoarrays, and ionic liquids (ILs) used for molecularly imprinted polymerization. The current variation for NSE obtained from the IL-based MIP sensor showed an apparent difference over other 7 interferents, although the signal of human serum albumin (HSA) was in half of that of the target. The reported sensor also presented good sensing performances in stability, sensor-to-sensor, and single electrode reproducibility with RSD values less than 5% [23]. Compared with Prizada et al., the IL-based MIP sensor offered a similar range of detection, but a lower LOD of 2.6 pg/mL. Recoveries ranging from 96.7% to 102.9% with RSD values less than 5% were indicated the IL-based MIP sensor could be used for clinical diagnosis. Same as NSE, neural cell adhesion molecule 1 (NCAM1), as so-called CD56, is regarded as another essential biomarker in SCLC. The increase of CD56 is a more persuasive signal to define SCLC because of its ability to significant expression in the body [39,40]. Ma et al. [24], provided a MIP-based electrochemical sensor for sensitive detection of CD56. A wider range of detection (i.e., 0.001 ~ 1 ng/mL) with an ultralow LOD of 0.47 pg/mL was achieved probably due to the use of sandwich-like multi-signal amplification. However, peer reports on detection of CD56 using MIP-based electrochemical sensor was not reviewed in a broader range except the comparison with a traditional probe-type sensor fabricated by the current study group [24].

The amount of carcinoembryonic antigen (CEA) is of great significance in diagnosis of colorectal cancer. MIP-based electrochemical sensing methods to this cancer biomarker has been received increasingly attention in recent years. Qi et al. [26], integrated microfluidic strategy with MIP technique to provide a paper-based electrochemical sensor for determination of CEA (Fig. 2c). The sensor displayed good reproducibility and room-temperature stability. Selectivity test was performed by mixing CEA with other 2 interfering substances, and acceptable results were acquired. Such creation can be further developed into commercially available homecare products, opening a promising way toward the

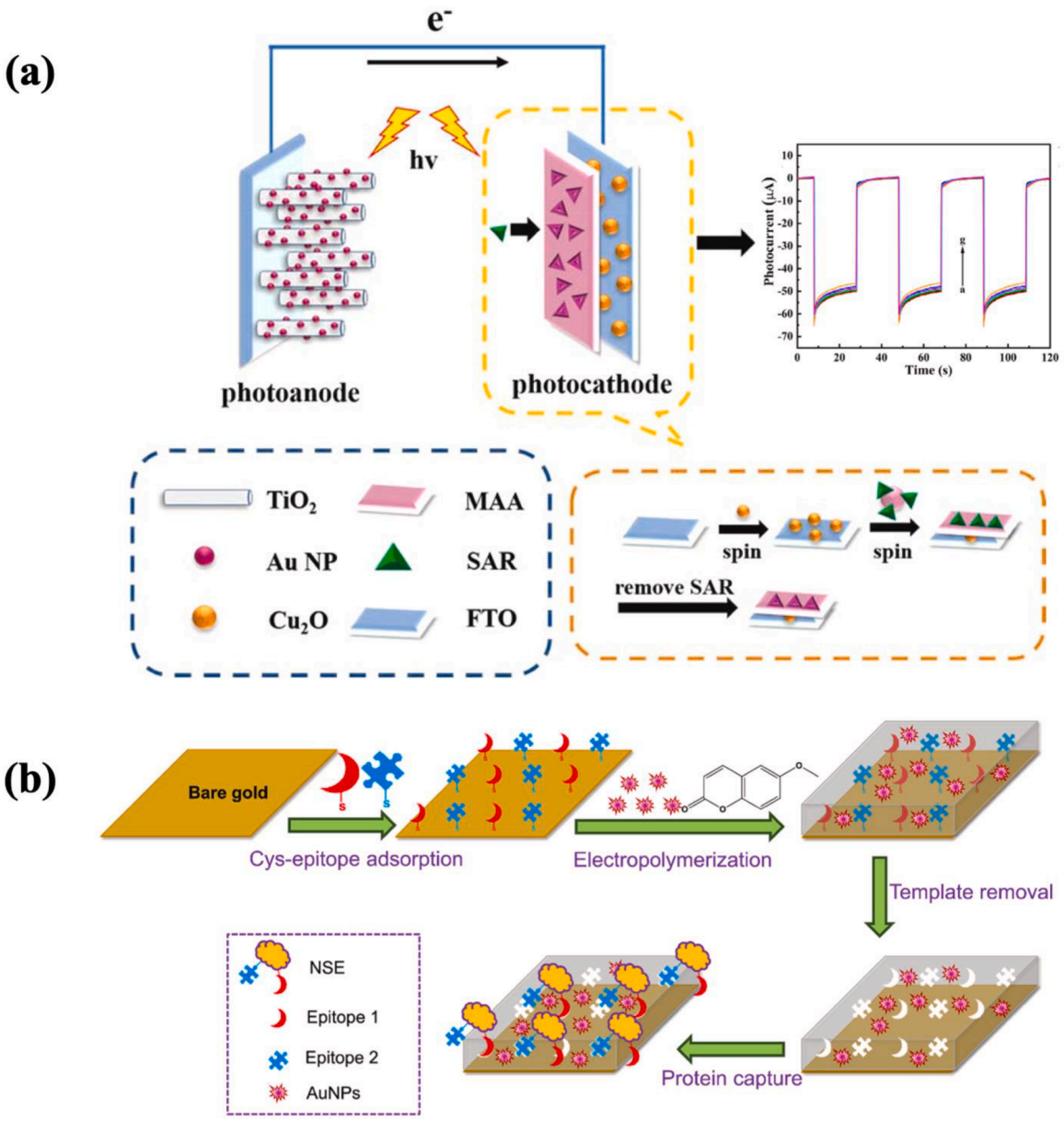

Fig. 1. Schematic diagrams of: (a) the photoelectrochemical cathodic MIP sensor for sensitive photocurrent-based determination of SAR. Reprinted from Sun et al. [21] (b) the epitope-suited MIP-based electrochemical sensor for selective detection of NSE. Reprinted from Pirzada et al. [22].

point-of-care monitoring because of low-cost, disposable, and miniaturized natures [16]. Carneiro et al. [25], created a passive direct methanol fuel cell (DMFC) for electrochemical sensing of CEA. The DMFC/MIP sensor enabled to yield a broader dynamic range of 0.1 ~ 100,000 ng/mL and a lower LOD of 80 pg/mL, along with high selectivity and reproducibility, in comparison to other MIP-based electrochemical sensors reviewed in the literature and the one presented by Qi et al. Power-current density plotting showed a satisfying discrimination against different concentrations of CEA when the sensor was tested in both standard buffer and serum solution. As seen in Fig. 2a, such self-powered sensor, exhibiting strong portability, which can highly promote the development of completely autonomous electrochemical setup especially in a sensor combined with a fuel cell [25].

The rapid spread of coronavirus disease 2019 (COVID-19) has been causing serious crises of public health, high medical pressure, and tremendous economic loss worldwide. Therefore, convenient, fast, and low-cost testing kits that can be massively produced are in an urgent demand to reduce the pressure of hospitals and spread of the pandemic. Severe acute respiratory syndrome coronavirus 2 (SARS-CoV-2) related biomolecules are the main biomarkers revealing the infection of the coronavirus [27]. Tabrizi et al. [27] prepared an analyte-specific MIP sensor on a macroporous gold deposited screen-printed electrode (SPE) for direct monitoring of the SARS-CoV-2-receptor binding domain (SARS-CoV-2-RBD) in saliva diluted with same-volume PBS solution. EIS measurement was performed showing discriminatory linear responses ranging from 0.002 ~ 0.04 ng/mL, as well as a LOD of 0.7 pg/mL. Although the sensor processed excellent sensitivity, selectivity, and stability, some disadvantages were also mentioned: one is the EIS monitoring always costly over other potentiostat-based methods, the other is the current sensor made of hard substrates cannot be developed into a wearable sensor [27]. Ayankojo et al. [28] fabricated a gold-thin-film metal electrode (Au-TFME) with the immobilization of imprinted caves for sensitive confirmation of the SARS-CoV-2 spike protein subunit S1 (ncovS1) in both PBS and actual nasopharyngeal samples from infected patients (Fig. 2b). With convinced selectivity and reproducibility, the sensor was further tested in the presence of other

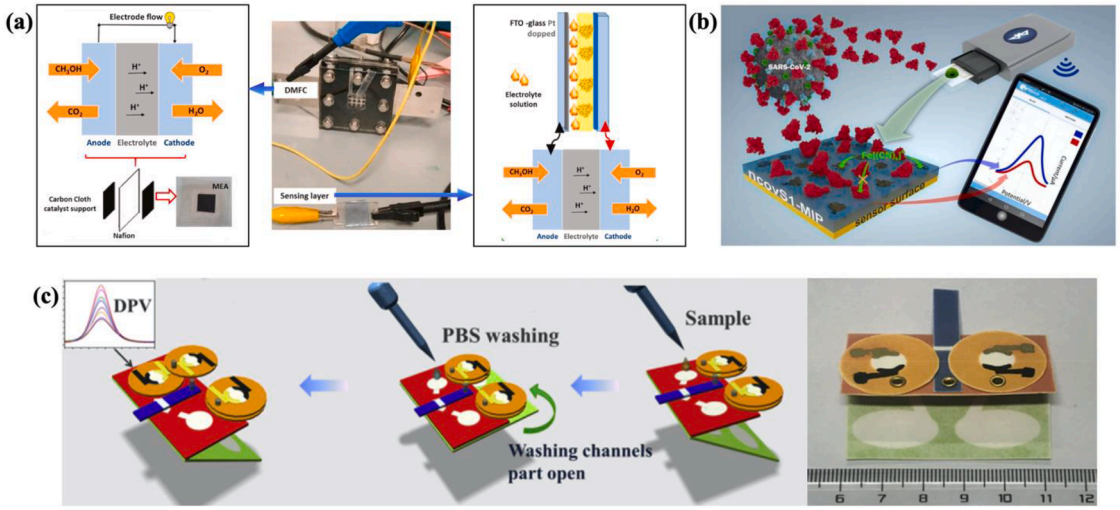

Fig. 2. (a) Working mechanism of the DMFC/MIP sensor used for detection of CEA, along with a real image of the device. Reprinted from Carneiro et al. [25] (b) the lab-on-chip Au-TFME/MIP sensor applied for sensitive monitoring of ncovS1. Reprinted from Ayankojo et al. [28] (c) the paper-based MIP electrochemical sensor integrated with microfluidic strategy for determination of CEA, along with a real image of the device. Reprinted from Qi et al. [26].

mutated strains of SARS-CoV-2 to critically assess the recognition towards the analyte. Results showed the sensor exhibited the highest affinity to ncovS1 over other mutated strains, verifying strong practicability in real specimens. Following the real testing requirement, the proposed sensor was connected to a hand-size potentiostat analyzer wirelessly connected to a mobile phone via Bluetooth. Apparent differences among the negative, negative spiked with ncovS1 in the lowest detectable concentration, and positive sample were observed, where the results were in accordance with those obtained from the research-grade device [28].

In fact, there are only a small number of MIP-based sensors integrated with handheld analyzers, while the rest of the sensors reported, at least for the present, are only suitable for laboratorial research because they always require to be connected to the analyzers that have not been miniaturized yet. Hence, several research groups tend to put significant effort on filling in the blank, by which the electrochemical MIP sensors prepared were usually with a better handheld appearance, showing stronger possibility of customization and commercialization.

A lab-on-chip determination of propofol in human plasma making use of molecularly imprinted cavities was reported by Hong et al. [41] A microfluidic system was constructed through well-patterned double-sided stickers layering between two blank cyclic olefin copolymer (COC) chips, as shown in Fig. 3b. Sample solution at microvolume was then precisely loaded into the sensing cells by virtue of capillary attraction, as presented in Fig. 3c and e. The as-fabricated MIP sensor was allowed to be integrated with a portable hand-sized analyzer (Fig. 3a), presenting voltage responses varying as a function of time to achieve the sensitive detection of propofol, as seen in Fig. 3d and f. The reported sensor had a rapid analyzing time of 25 s. Blood samples from the hospital were centrifuged for 20 min to separate the plasma and used for the real sample testing. EIS-based measurement was performed showing the binding of propofol saturated at around 20 s. Although the sensor reached a determination range of 100 $\sim$ 3 $\times$ 10^4 ng/mL, with a LOD of 10^5 pg/mL, there was no peer review on detection of propofol in real biofluids using MIP-based electrochemical sensors. Moreover, future development regarding this microfluidic chip-based MIP sensor was also claimed in the paper according to the current progress. A microfiltration component is expected to be added in the setup for effective elimination of any bio-impurities that may interfere electrical sensing signals especially in the event of whole blood testing. Also, it is desirable to install a negative-pressured part for high-quality enrichment of plasma, rather than the centrifugation of raw blood sample at

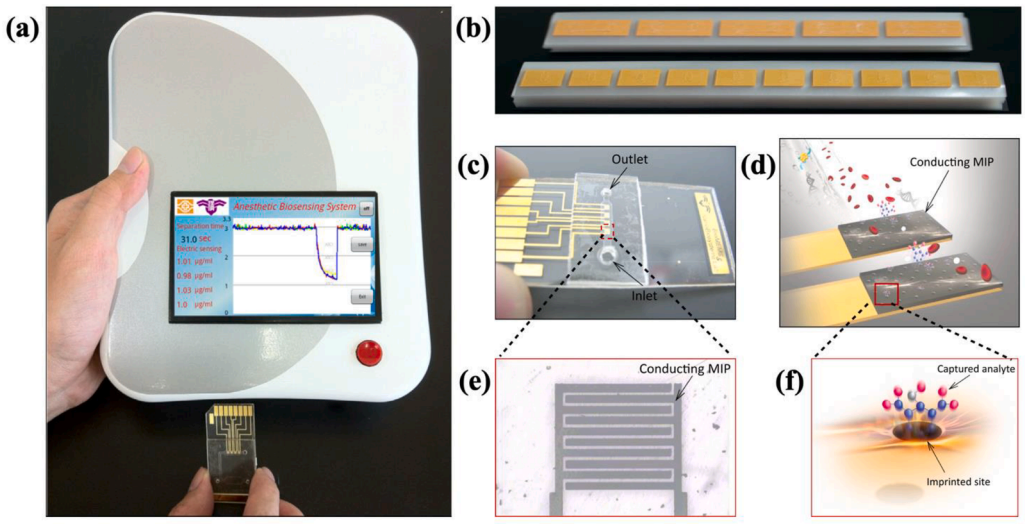

Fig. 3. Microfluidic chip based electrochemical MIP sensor for determination of propofol: (a) real photograph of the MIP sensor inserted into a handheld analyzer. (b) microfluidic stickers used for the microchannel creation. (c) microfluidic chip with the embedded MIP functional layer. (d) target molecules rebinding to the MIP-based sensing surface. (e) enlarged image of the conductive MIP coverage on the gold interdigitated array microelectrode (IDA). (f) enlarged schematic diagram of molecularly imprinted cavities recognizing the specific target analyte propofol. Reproduced from Hong et al. [41].

hospital laboratories [41].

As mentioned in many paper, electrochemical sensors integrated with microfluidic strategy is regarded as a promising platform for point-of-care sensing with merits of controllable sample volume, cost effectiveness, and device portability. It cannot be denied that microfluidic components possess overwhelming capability of autonomous sampling through intrinsic capillary action.

Wang et al. [42], combined this advantage with a wearable sensing patch, aiming to realize an on-site and real-time personalized health monitoring (Fig. 4a). The sensing patch allowed various metabolites in sweat samples to be specifically recognized through delicate imprinted cavities and to yield electrochemical responses with the synergistic effect of redox-active nano-reporters (RARs) and laser-engraved graphene (LEG) (Fig. 4b). Sensing outcomes were transferred through Bluetooth into a programmed software (i.e., NutriTrek) displayed at a mobile phone (Fig. 4c). Moreover, the research group also launched a ready-for-market product of smartwatch incorporating the essential wearable MIP sensing patch, which reached a more advanced technical level over other reported MIP-based sensing devices (Fig. 4d). This work featured the first real-time wearable sensing based on a MIP detection mechanism as the previously reported sensing platforms mostly suffered from vigorous washing steps to regenerate imprinted polymeric receptors [42]. This versatile microfluidic MIP sensor enabled successful monitoring of amino acids (AAs) such as tyrosine (Tyr) and tryptophan (Trp), as well as some branched-chain amino acids (BCAAs) like leucine (Leu), isoleucine (Ile), and valine (Val).

The proposed sensing surface could be facilely modified: on one hand, only LEG was deposited at the bottom of the MIP interface to directly react with Tyr-and Trp-because of their electroactive nature (Fig. 4e). The sensing process was measured using classic DPV technique. On the other hand, LSV-based indirect determination conducted on the composition of MIP/RAR/LEG (layers from top to bottom) was applied to monitor the BCAAs since they were not electroactive but could serve as an electron shield to avoid RARs being exposed to the sample environment (Fig. 4g). Regeneration of cavities in this sensor could be manually controlled by altering electrical parameters without any washing step (Fig. 4f and h). Apart from the basic amino acids, the wearable sensor enabled to determine an extremely wide range of organic substances [42]. Furthermore, the sensor had the ability to capture different types of target molecules at a single sensing area due to the powerful multi-template MIP scheme (Fig. 4i). The combination of those unique sensing components (i.e., MIP/RAR/LEG) made the sensor have outstanding capability of cavity regeneration in a raw biological specimen (i.e., human sweat) (Fig. 4j). On-site analysis based on real sweat liquid are more complicated than the ones tested in standard buffered solutions owing to the multiple bio-constituents. Therefore, the presented setup was equipped with accurate electrochemical methodologies coupled to a timely temperature/electrolyte calibrating functionality to achieve sensitive real-time sweat sensing (Fig. 4k).

To further enhance the applicability of the sensor, sweat secretion stimulated at rest durations and the sample collection were regarded as their next concerns. The volume of sweat at sedentary situation is normally negligible compared with the one right after physical exercise, therefore of great difficulty in collecting the measurable amount of sweat under calmness. To overcome this challenge, carbachol was eventually selected as a novel muscarinic agent for continuous microsampling of sweat rather than traditional pilocarpine [42]. The research group presented a schematic contract between carbachol and pilocarpine with their influences on sweat glands (Fig. 4l), showing a bright comparison that carbachol could provide a more efficient sweat collection ascribed to its extra nicotinic effects [43]. In their actual measurements, a dramatically reduced current (i.e., around 15–20 times smaller than that was commonly applied in other studies [44]) was used to approach the goal of safe on-body monitoring with imperceptible skin

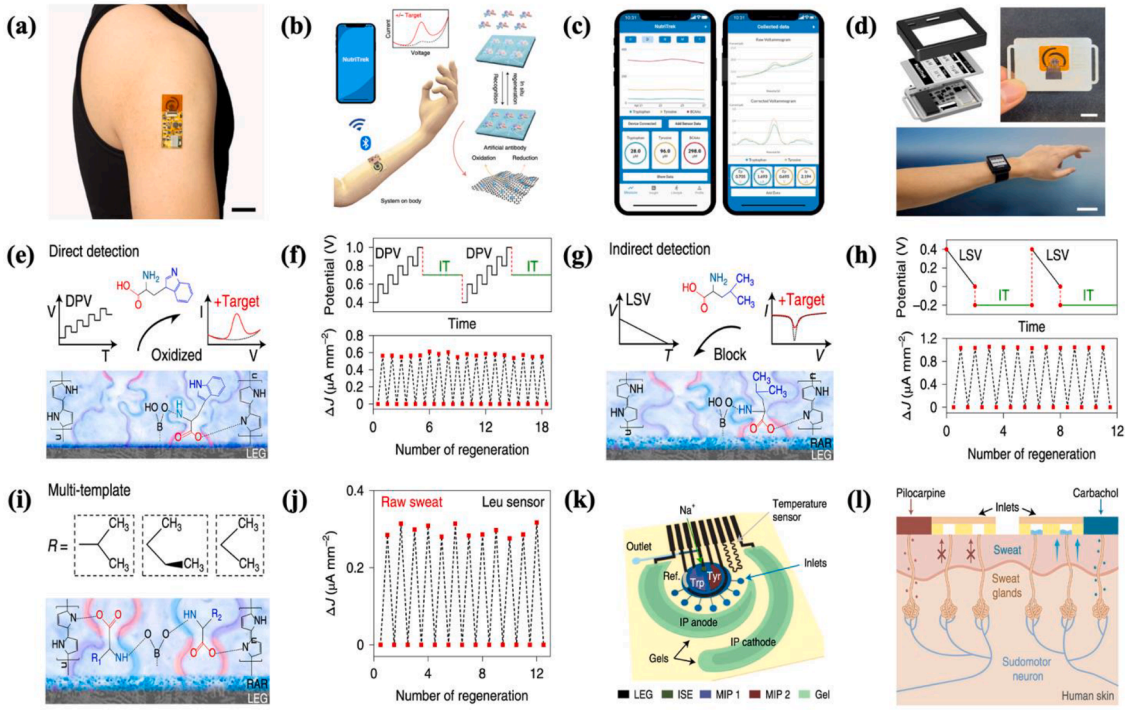

Fig. 4. Wearable sweat-sampling electrochemical MIP sensor used for on-site and timely health monitoring: (a) wearable sensing patch in practical use; (b) components contributed to the sensor and its working mechanism; (c) mobile phone-based data presenting; (d) smartwatch containing the MIP sensing patch; (e) schematic illustration of direct detection of electroactive substances based on MIP/LEG; (f) cavity regeneration through DPV-related manipulation; (g) schematic illustration of indirect detection of non-electroactive substances based on MIP/RAR/LEG; (h) cavity regeneration through LSV-related manipulation; (i) schematic illustration of multiple target detection based on MIP/RAR/LEG; (J) cavity regeneration realized in raw sweat samples; (k) schematic representation of the real-time sweat sensing device equipped with a timely temperature/electrolyte calibrating functionality; (l) schematic contract between carbachol and pilocarpine with their influences on sweat glands. Reproduced from Wang et al. [42] with permission from Nature Biomedical Engineering.

irritation. Additionally, high levels of BCAAs usually imply the potential risk of suffering insulin-resistant obesity and metabolic syndrome, among which the increased level of Leu-has been confirmed that it has a close correlation to COVID-19 infection [42].

Conclusively, this wearable MIP-based electrochemical sensor compiles a variety of advantages, meanwhile, it avoids repeatedly appeared shortcomings of many other contemporaneous MIP-based sensing devices. For example, the proposed sensor allows clinical trials to be performed using untreated biological fluids; it also exhibits strong reusability in multicycle analyses because the imprinted polymeric traps can be electrochemically regenerated after each type of analyte rebinding; micro-volume sampling can be realized on this sensor through the capillary effect which is originated from microfluidic accessories; broad range of application with respect to the sensor from real-time monitoring of organic nutrient, early diagnosis of disease, to sensitive warning of virus infection. The integration of electrochemical MIP sensor with microfluidic system is demonstrated again to be a highly feasible sensing composition for in-situ and point-of-care applications.

Cardiac troponin I (cTnI) plays a critical role in the contraction of myocardial muscles [45]. This substance always can be detected in serum when the myocardium is impaired [46], thus it always considered as the typical biomarker representing acute myocardial infarction [47]. Zhang et al. [29], developed a $CuFe_2O_4$ nanoparticle-based MIP sensor for determination of cTnI in human serum (Fig. 5a). Magnetic nanoparticles were effectively adsorbed on the electrode surface to increase the sensitivity [48]. The dual-mode sensor could yield both electrochemical and colorimetric response towards the analyte, along with favorable selectivity, signal reproducibility, and stability. He et al. [30], reported a MIP-coated electrode for simultaneous detection of cTnI and myoglobin (Mb) based on an electrochemiluminescence immunoassay (Fig. 5b). Interestingly, same sensing strategies as sandwich-type analyte recognition and signal amplification were presented in these two papers. The sensors exhibited similar detection ranges. However, a lower LOD of 3.2 pg/mL was obtained from the one provided by Zhang et al. probably due to the use of nano-scaled MIP in their work [29]. NanoMIP sensors belong to a unique derivative of MIP-based sensors, where the analyte-recognition caves are normally created on nanomaterials (e.g., nanoparticles) instead of the traditional imprinted cavities generated at bulky polymeric layers, thus offering higher surface area, affinity, and sensitivity to target molecules in sensing applications.

2.2. *Body-produced chemicals and hormones detected using MIP-based electrochemical sensors*

Glucose is a vital chemical to participate several important life activities in living bodies. One of the activities is being as a typical indicator for sugar levels in blood serum. Glucose that cannot be effectively transformed into its metabolites by insulin is prone to resulting in an elevation of sugar level, causing diabetes mellitus (DM) [59]. Therefore, it is highly necessary to develop a convenient and sensitive platform for glucose detection in body fluids.

Yang et al. [51], reported a novel method to the fabrication of MIP-based sensors by electrodeposition of molecularly imprinted

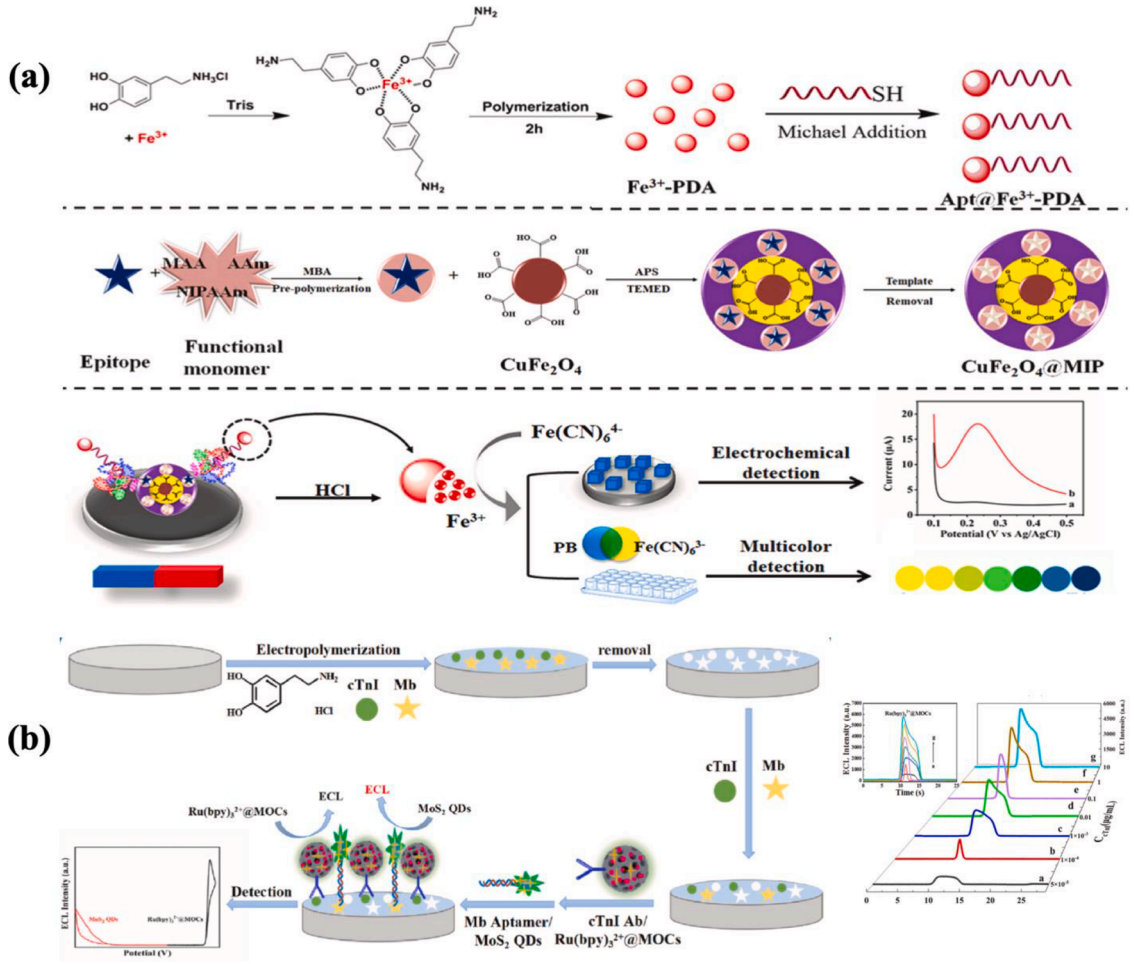

Fig. 5. Schematic illustrations of: (a) the dual-mode CuFe2O4 nanoparticle-based MIP sensor used for detection of cTnI in human serum. Reprinted from Zhang et al. [29] (b) the MIP-based ECL sensor applied for simultaneous detection of cTnI and Mb. Reprinted from He et al. [30].

polymeric micelles (MIPMs) and photo-crosslinking of the amphiphilic copolymer (Fig. 6a). The obtained sensor exhibited good selectivity, stability, and signal reversibility toward glucose, owing to the robust recognition cavities. However, the dynamic range and LOD were mainly lying in high concentrations, same as those presented in Diouf et al. [50] Also, the sensor reproducibility was imperfect from batch to batch due to the use of homemade copolymer and MIPMs [51]. Sehit et al. [49], provided a facile MIP-based electrochemical sensor decorated only with gold nanoparticles (AuNPs) for sensitive detection of glucose. The sensor yielded a lower LOD compared with those shown in Yang et al. and Diouf et al. With acceptable selectivity, specificity, and stability, the sensor was applied to detect glucose in both diluted human serum samples and undiluted ones. Recoveries ranging from 93.8% to 95% with RSD $< 8\%$ were achieved in undiluted cases, revealing a strong applicability in real biological environment [49]. Instead of blood samples collected for glucose detection, Diouf et al. [50], aimed to seek an alternative of blood, such as saliva, to achieve similar results. This opens a new avenue to the non-invasive testing, although the determination range as well as LOD reported in the literature were not highly sensitive.

Cholesterol (CHO) is one of body products that plays as an important precursor for synthesis of hormones as well as other vital substances, supporting many biological functions in living creatures. However, CHO always with a high level in blood serum can result in hypercholesterolemia, which is considered as the primary inducement of atherosclerotic cardiovascular diseases (ASCVDs) [60]. Because of good selectivity and reproducibility, Ji et al. [52], showed a wider dynamic range and a lower LOD in comparison to other recently reported papers. The shelf life of the sensor was also evaluated after 10 and 30 days, leaving no significant change and 91.68% of the initial response, respectively. However, there was no data regarding the applicability in actual clinical analysis of the sensor, the study group claimed this part of work required to be intensively studied in a long period [44]. Yang et al. [53], further improved the sensing ability of MIP-based sensors towards CHO at the basis of Ji et al. and received a broad detection range of $3.87 \times 10^{-10} \sim 3.87 \times 10^{-5}$ ng/mL along with an ultralow LOD of 1.3×10^{-7} pg/mL. Performances like selectivity, reproducibility and stability of the proposed device were also highly competitive over other previously reported MIP-based sensors. Real testing was performed by adding CHO with femtomolar level in human serum, resulting in recoveries varying from 97% to 100.4% with small RSD (i.e., 1.7%) [53].

Neurotransmitters are another class of important body-produced chemicals, which also play significant roles in endocrine and central nervous system. Dopamine (DA) and epinephrine (EP) are typical neurotransmitters produced in mammals. The detection of these neurotransmitters usually presented insensitive results due to their high structural similarity as well as the coexistence nature in real body fluids [61,62,63]. To tackle this issue, Fetma et al. [55], constructed a special MIP-based sensor where the SPE electrode was modified with acryloylated-graphene oxide / carbon black (aGO/CB), forming a cross-linking functional monomer that could be polymerized into dual-type imprinted cavities for simultaneous determination of DA and EP (Fig. 6b). The sensor had the capability of determining the analytes in both aqueous and biological fluids (i.e., blood serum and urine) with high analyte specificity. Real samples used in their work were only

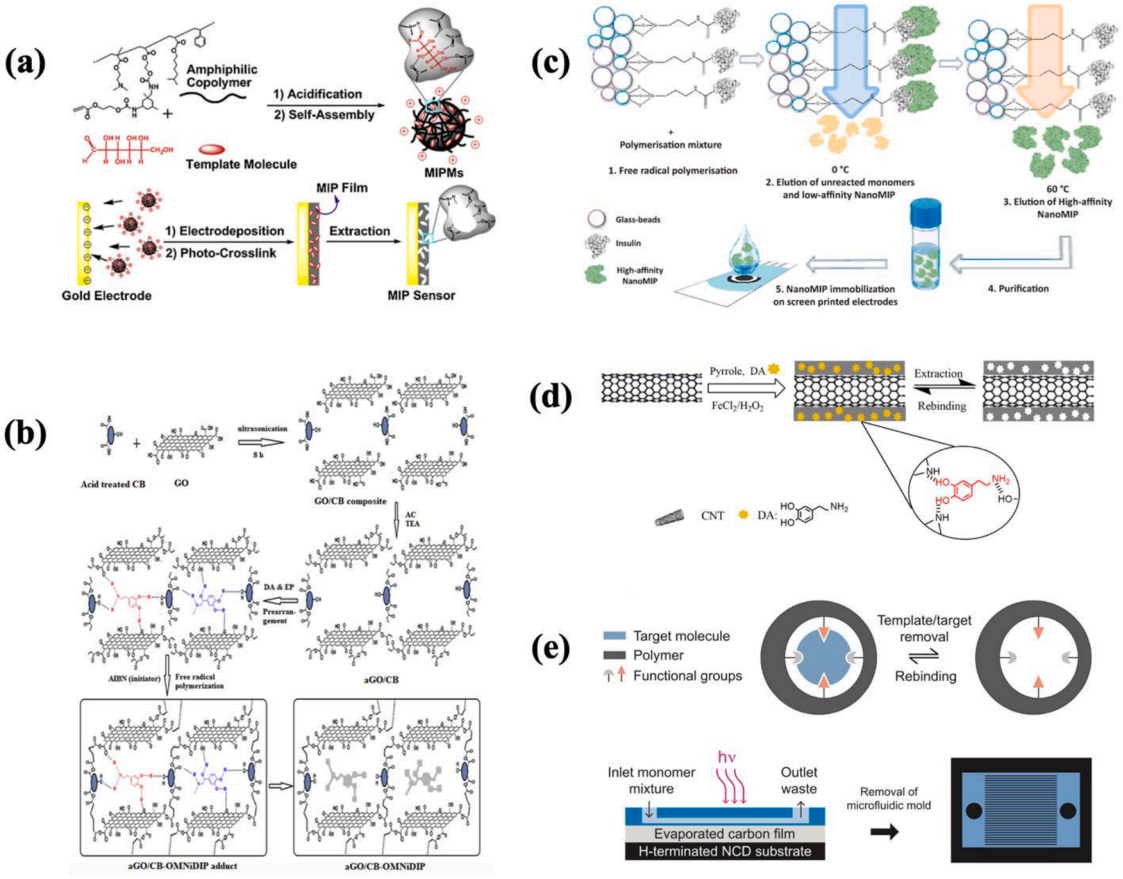

Fig. 6. Schematic representation of: (a) the gold electrode supported MIPM sensor used for detection of glucose. Reprinted from Yang et al. [51] (b) the aGO/CB based MIP-based electrochemical sensor with two types of analyte-specific cavities used for simultaneous detection DA and EP. Reprinted from Fetma et al. [55] (c) the SPE modified with nanoMIPs as the recognition element for determination of insulin. Reprinted from Cruz et al. [56] (d) the carbon nanotube-based MIP sensor applied for determination of DA Reprinted from Qian et al. [54] (e) the MIP-based sensor fabricated using microfluidics and in situ photo-polymerization for detection of testosterone. Reprinted from Kellens et al. [58].

diluted in a proper volume ratio with absence of any other pretreatments aiming to increase the accuracy at trace amount of detection [55]. Same as Zhang et al., Qian et al. [54], achieved the sensitive monitoring of DA relying on carbon nanotube-based MIPs (Fig. 6d). A wider detection range of $7.659 \times 10^{-3} \sim 765.9$ ng/mL, as well as a lower LOD of 1.53 pg/mL was realized on the proposed sensor compared with the results presented by Fetma et al. and good recoveries coupled with reasonable RSD values were also obtained from the real sample testing using the as-prepared sensor [54].

Sensitive determination towards hormones is highly important for early recognition of diseases and health monitoring. There are a growing number of reports showing interest in hormone detection. Cruz et al. [56], reported a nanoMIP electrochemical sensors where the polymeric nanoparticles were well-designed to form imprinted chambers for specific binding to insulin (Fig. 6c). Owing to the negligible cross-reactivity, the sensor enabled to provide a detection limit of 0.464 pg/mL in real human plasma, which was approximately 20 times lower the LOD (i.e., 8.593 pg/mL in human serum) obtained from a lab-on-paper aptasensor fabricated by Niroula et al. [64], further demonstrating the high sensing performances of nanoMIP sensors. Moreover, the long-term stability was also evidenced by storing 7 sensors at 4 °C place and measured them in weekly intervals, leaving a drop of only 35% of initial response after 168 days. Peer review regarding the determination of insulin level using MIP-based electrochemical sensors was also presented in the paper, showing the nanoMIP strategy capable of detecting insulin with highly competitive sensing performances in comparison to other reported devices [56].

Testosterone is an essential hormone in charge of regulating many male characteristics. Inadequate level of testosterone increases the risk of suffering high-grade prostate cancer and cardiovascular diseases [65, 66]. On the other hand, testosterone is defined as one of common doping chemicals, which has been prohibited by the World Anti-Doping Agency (WADA) from using in sports events [67]. Hence, there is an urgent need to develop a monitoring system for sensitive detection of testosterone. Kellens et al. [58], fabricated an amount controllable MIP interface making use of a well-patterned microfluidic template, to reach the detection of testosterone in buffer in combination with electrochemical impedance spectroscopy (EIS), exhibiting good linear responses from 0.144 to 5.76 ng/mL with a LOD of 144 pg/mL (Fig. 6e). The sensor was allowed to detect the structural analogues of testosterone (i.e., estriol and β-estradiol) to assess the selectivity. β-estradiol, to some extent, presented affinity towards the MIP interface due to the steric similarity to testosterone, while estriol showed the largest structural difference from testosterone resulting in negligible responses. Furthermore, the applicability of the sensor was evaluated by detecting testosterone in urine and saliva samples. Sensor performances obtained from the salivary solution were not good as the ones yielded from buffer and urine, which may be ascribed to the incomplete pretreatment of saliva, leaving residual proteins or other biomolecules that prevent testosterone from binding to the polymeric cavities [58]. Liu et al. [57], highly improved the sensing ability towards testosterone through a glassy carbon electrode (GCE) modified with graphene oxide (GO) and MIP, receiving a wider detection range of $2.88 \times 10^{-7} \sim 288.42$ ng/mL with an ultralow LOD of 1.15×10^{-4} pg/mL, compared with the ones showed in Kellens et al. and other recent reports. Excellent analyte selectivity was approved by testing testosterone as well as other 3 structurally similar interferents and 4 endogenous substances. Signal repeatability, electrode-to-electrode reproducibility, and long-term (i.e., up to 30 days storage) stability were also confirmed with desirable results. Moreover, this MIP/GO electrochemical sensor also presented a strong regeneration capability by washing the used sensor with ethanol solution and reached a signal recovered by 96.2%. Real sample analysis was performed in human serum and recoveries ranging from 98.6% to 104.2% with RSD values smaller than 4.82% was obtained, indicating the satisfying applicability of the proposed sensor, which was indeed a good MIP-based electrochemical sensor for ultrasensitive determination of testosterone [57].

3. Conclusions and perspectives

Sensitive sensors that can screen health conditions in real time are of great helpful for timely intervention of diseases, development of telemedicine, as well as advanced homecare. MIP-based sensors introduce single- or dual- type of functional monomers to create analyte-preferred polymeric receptors, with high regeneration rate through simple electrochemical manipulation. Such recognition elements are sometimes also called 'artificial antibodies' due to the similar binding mechanism to the antibody-antigen conjugation. MIP-based electrochemical sensors possess valuable properties of prolonged lifetime, capability of homo- or hetero- shaped cavity design, and less impact by the ambient environment (e.g., temperature), which has attracted increasing attention in comparison to traditional electrochemical immunosensors. Nevertheless, majority of papers elucidate the development of sensors mainly in the following two aspects: one is to introduce a novel surface modification for MIP-based electrodes to achieve the purpose of research innovation, the other is to perform electrochemical determination of a new substances replying on the MIP-based electrode produced with old-fashioned techniques. Compared with the attention towards the laboratory-scaled studies on electrochemical MIP sensors, the ones in relation to the evaluation on sensing maturity of sensors are rarely reported. Although the experimental works reported in papers include sensing signal recovery tests in real biological samples, most of which merely employ the standard analyte-spiked method or perform the assay in synthetic biofluids that already have an initial concentration, which still leave a long distance to reach a direct use of body-produced fluids collected on-site for real-time application.

Sensors among which integrate the MIP technique with electrochemical monitoring have been developed for a few decades [68]. However, there are still many issues required to be urgently addressed in this field according to the papers reported:

1. Body fluids such as human serum, plasma, saliva, and urine, are required to be properly diluted prior to performing assays in actual biological environments on electrochemical MIP sensors. Extra scientific operations like vortex mixing, centrifugation, and microfiltration, are often needed especially for the fluids containing numerous biomolecules, aiming to achieve a qualified sample solution before analysis. Future investigation could be focusing on the development of the MIP-based sensors suitable for being tested in undiluted conditions.
2. Some electrodes (e.g., SPE) used in MIP-based electrochemical sensors have great potential of mass production. However, most articles only present a summarized description on the fabrication process and raw materials for electrode preparation but lack a detailed manufacture workflow specific to the massive production in industrial lines and batch-to-batch quality assessment.
3. At present, MIP-based electrochemical sensors with limited smartness still account for a large proportion. Further attempts might include the improvement of the device autonomous capability such as the self-controlled 'sample loading – sensing – electrode surface washing'. Such cyclical monitoring could be achieved by applying a software that is set in an automatic mode.
4. Laboratory-grade sensing devices often lack adequate exploration on their portability according to recent advances on electrochemical MIP sensors. Desirable portability often equips with two characteristics, namely a miniaturized working electrode (i.e., the one modified with molecularly imprinted polymeric recognitions) and a handheld analyzer for data presenting and processing.

Up to present, commercial products with respect to electrochemical MIP sensors are still rarely reported. Therefore, more attention might be paid at the later stage of laboratorial research, including success

probability of the sensors used in real clinical applications, transfer to large-scale industrial production, economic effectiveness after flowing into markets, and user experience and satisfaction.

Declaration of Competing Interest

The authors declare that they have no known competing financial interests or personal relationships that could have appeared to influence the work reported in this paper.

Data availability

No data was used for the research described in the article.

Acknowledgement

Mr Matthew Pagett would like to acknowledge the financial support from EPSRC DTP program for his PhD scholarship (Ep/R51312x/1).

References

[1] K. Murugan, V.K. Jothi, A. Rajaram, A. Natarajan, ACS Omega 7 (2021) 1368–1379.
[2] Y. Hu, X. Lu, J. Food Sci. 81 (2016) N1272–N1280.
[3] J. Ashley, Y. Shukor, R. D'Aurelio, L. Trinh, T.L. Rodgers, J. Temblay, M. Pleasants, I.E. Tothill, ACS Sens. 3 (2018) 418–424.
[4] G. Ertürk Bergdahl, T. Andersson, M. Allhorn, S. Yngman, R. Timm, R. Lood, ACS Sens. 4 (2019) 717–725.
[5] M. Sundhoro, S.R. Agnihotra, N.D. Khan, A. Barnes, J. BelBruno, L. Mendecki, Sci. Rep. 11 (2021) 1–9.
[6] M.M. El-Wekil, H.M. Halby, M. Darweesh, M.E. Ali, R. Ali, Sci. Rep. 12 (2022) 1–9.
[7] S. Krishnan, J. Electrochem. Soc. 167 (2020), 167505.
[8] L. Wang, H. Wang, C. Tizaoui, Y. Yang, J. Ali, W. Zhang, Sens. Diagn. 2 (2023) 46–77, 2023.
[9] W. Zhang, M.B. Dixon, C. Saint, K.S. Teng, H. Furumai, ACS Sens. 3 (2018) 1233–1245.
[10] W. Zhang, L. Wang, Y. Yang, P. Gaskin, K.S. Teng, ACS Sens. 4 (2019) 1138–1150.
[11] M. Pagett, K.S. Teng, G. Sullivan, W. Zhang, Glob. Chall. 7 (2023), 2200093.
[12] G. Premaratne, J. Niroula, M.K. Patel, W. Zhong, S.L. Suib, A.K. Kalkan, S. Krishnan, Anal. Chem. 90 (2018) 12456–12463.
[13] G. Premaratne, S. Farias, S. Krishnan, Anal. Chim. Acta. 970 (2017) 23–29.
[14] L. Wang, W. Zhang, S. Samavat, D. Deganello, K.S. Teng, ACS Appl. Mater. Interface. 2020 12 (31) (2020) 35328–35336.
[15] S. Samavat, J.S. Lloyd, L. O'Dea, W. Zhang, E. Preedy, S. Luzio, K.S. Teng, Biosens. Bioelectron. 118 (2018) 224–230.
[16] W. Zhang, B. Jia, H. Furumai, Sci. Rep. 8 (2018) 10686.
[17] W. Zhang, C. Han, B. Jia, C. Saint, M. Nadagouda, P. Falaras, L. Sygellou, V. Vogiazi, D. Dionysiou, Electrochim. Acta 236 (2017) 319–327.
[18] A. Yarman, S. Kurbanoglu, K.J. Jetzschmann, S.A. Ozkan, U. Wollenberger, F. W. Scheller, Curr. Med. Chem. 25 (2018) 4007–4019.
[19] A. Yarman, S. Kurbanoglu, I. Zebger, F.W. Scheller, Sens. Actuators B Chem. 330 (2021), 129369.
[20] O. Sheydaei, H. Khajehsharifi, H.R. Rajabi, Sens. Actuators B Chem. 309 (2020), 127559.
[21] J. Sun, Y. He, S. He, D. Liu, K. Lu, W. Yao, N. Jia, Biosens. Bioelectron. 204 (2022), 114056.
[22] M. Pirzada, E. Sehit, Z. Altintas, Biosens. Bioelectron. 166 (2020), 112464.
[23] X. Wang, Y. Wang, X. Ye, T. Wu, H. Deng, P. Wu, C. Li, Biosens. Bioelectron. 99 (2018) 34–39.
[24] X. Ma, M. Li, P. Tong, C. Zhao, J. Li, G. Xu, Biosens. Bioelectron. 156 (2020), 112150.
[25] L.P. Carneiro, N.S. Ferreira, A.P. Tavares, A.M. Pinto, A. Mendes, M.G.F. Sales, Biosens. Bioelectron. 175 (2021), 112877.
[26] J. Qi, B. Li, N. Zhou, X. Wang, D. Deng, L. Luo, L. Chen, Biosens. Bioelectron. 142 (2019), 111533.
[27] M.A. Tabrizi, J.P. Fernández-Blázquez, D.M. Medina, P. Acedo, Biosens. Bioelectron. 196 (2022), 113729.
[28] A.G. Ayankojo, R. Boroznjak, J. Reut, A. Öpik, V. Syritski, Sens. Actuators B Chem. 353 (2022), 131160.
[29] G. Zhang, L. Zhang, Y. Yu, B. Lin, Y. Wang, M. Guo, Y. Cao, Biosens. Bioelectron. 167 (2020), 112502.
[30] S. He, P. Zhang, J. Sun, Y. Ji, C. Huang, N. Jia, Biosens. Bioelectron. 201 (2022), 113962.
[31] F. Jentzmik, C. Stephan, K. Miller, M. Schrader, A. Erbersdobler, G. Kristiansen, M. Lein, K. Jung, Eur. Urol. 58 (2010) 12–18.
[32] L. Yang, W.J. Zhu, X. Ren, M.S. Khan, Y. Zhang, B. Du, Q. Wei, Biosens. Bioelectron. 91 (2017) 842–848.
[33] Y. Zhang, X.W. Wang, L.S. Song, C.L. Xu, L.Y. Ma, Z.H. Li, J.Z. Xi, X.Y. Jiang, Anal. Method. 4 (2012) 3466–3470.
[34] R. Molina, S. Holdenrieder, J.M. Auge, A. Schalhorn, R. Hatz, P. Stieber, Cancer Biomark. 6 (2010) 163–178.
[35] P.J. Marangos, D.E. Schmechel, Annu. Rev. Neurosci. 10 (1987) 269–295.
[36] Z. Altintas, A. Takiden, T. Utesch, M.A. Mroginski, B. Schmid, F.W. Scheller, R. D. Süssmuth, Adv. Funct. Mater. 29 (2019) 1–11.
[37] R. Tchinda, A. Tutsch, B. Schmid, R.D. Süssmuth, Z. Altintas, Biosens. Bioelectron. 123 (2019) 260–268.
[38] J. Drzazgowska, B. Schmid, R.D. Süssmuth, Z. Altintas, Anal. Chem. 92 (2020) 4798–4806.
[39] M. Früh, D. De Ruysscher, S. Popat, L. Crino, S. Peters, E. Felip, ESMO guidelines working group, Ann. Oncol. 24 (s6) (2013) 99–105.
[40] K. Hiroshima, A. Iyoda, T. Shida, K. Shibuya, T. Iizasa, H. Kishi, T. Tanizawa, T. Fujisawa, Y. Nakatani, Mod. Pathol. 19 (2006) 1358–1368.
[41] C.C. Hong, C.C. Lin, C.L. Hong, Z.X. Lin, M.H. Chung, P.W. Hsieh, Biosens. Bioelectron. 86 (2016) 623–629.
[42] M. Wang, Y. Yang, J. Min, Y. Song, J. Tu, D. Mukasa, C. Ye, C. Xu, N. Heflin, J. S. McCune, T.K. Hsiai, Z. Li, W. Gao, Nat. Bio. Eng. 6 (2022) 1225–1235.
[43] B. Riedl, M. Nischik, F. Birklein, B. Neundörfer, H.O. Handwerker, J. Auton. Nerv. Syst. 69 (1998) 83–88.
[44] J. Kim, I. Jeerapan, S. Imani, T.N. Cho, A. Bandodkar, S. Cinti, P.P. Mercier, J. Wang, ACS Sens. 1 (2016) 1011–1019.
[45] M.F. Fathil, M.K. Md Arshad, S.C. Gopinath, U. Hashim, R. Adzhri, R.M. Ayub, A. R. Ruslinda, M.N.M. Nuzaihan, A.H. Azman, M. Zaki, T.H. Tang, Biosens. Bioelectron. 70 (2015) 209–220.
[46] P. Nandhikonda, M.D. Heagy, J. Am. Chem. Soc. 133 (2011) 14972–14974.
[47] S. Dhawan, S. Sadanandan, V. Haridas, N.H. Voelcker, B. Prieto-Simon, Biosens. Bioelectron. 99 (2018) 486–492.
[48] S. Krishnan, K.Y. Goud, Magnetochemistry 5 (2019) 64.
[49] E. Sehit, J. Drzazgowska, D. Buchenau, C. Yesildag, M. Lensen, Z. Altintas, Biosens. Bioelectron. 165 (2020), 112432.
[50] A. Diouf, B. Bouchikhi, N. El Bari, Mater. Sci. Eng. C. 98 (2019) 1196–1209.
[51] Y. Yang, C. Yi, J. Luo, R. Liu, J. Liu, J. Jiang, X. Liu, Biosens. Bioelectron. 26 (2011) 2607–2612.
[52] J. Ji, Z. Zhou, X. Zhao, J. Sun, X. Sun, Biosens. Bioelectron. 66 (2015) 590–595.
[53] H. Yang, L. Li, Y. Ding, D. Ye, Y. Wang, S. Cui, L. Liao, Biosens. Bioelectron. 92 (2017) 748–754.
[54] T. Qian, C. Yu, X. Zhou, P. Ma, S. Wu, L. Xu, J. Shen, Biosens. Bioelectron. 58 (2014) 237–241.
[55] S. Fatma, B.B. Prasad, S. Jaiswal, R. Singh, K. Singh, Biosens. Bioelectron. 135 (2019) 36–44.
[56] A.G. Cruz, I. Haq, T. Cowen, S. Di Masi, S. Trivedi, K. Alanazi, E. Piletska, A. Mujahid, S.A. Piletsky, Biosens. Bioelectron. 169 (2020), 112536.
[57] W. Liu, Y. Ma, G. Sun, S. Wang, J. Deng, H. Wei, Biosens. Bioelectron. 92 (2017) 305–312.
[58] E. Kellens, H. Bové, T. Vandenryt, J. Lambrichts, J. Dekens, S. Drijkoningen, J. D'Haen, W.D. Ceuninck, R. Thoelen, T. Junkers, K. Haenen, A. Ethirajan, Biosens. Bioelectron. 118 (2018) 58–65.
[59] K. Harikumar, G.J. Hemalatha, B. Kumar, S.F.S. Lado, IJNTPS 4 (2014) 201–217.
[60] N.O. Stitziel, S.W. Fouchier, B. Sjouke, G.M. Peloso, A.M. Moscoso, P.L. Auer, A. Goel, B. Gigante, T.A. Barnes, O. Melander, Arterioscler. Thromb. Vasc. Biol. 33 (2013) 2909–2914.
[61] F.H. Cincotto, T.C. Canevari, A.M. Campos, R. Landers, S.A.S. Machado, Analyst 139 (2014) 4634–4640.
[62] W. Ma, X. Yao, D. Sun, Asian J. Chem. 25 (2013) 6625–6634.
[63] L.C.S. Figueiredo-Filho, T.A. Silva, F.C. Vicentini, O. Fatibello-Filho, Analyst 139 (2014) 2842–2849.
[64] J. Niroula, G. Premaratne, S. Krishnan, Biosens. Bioelectron. X. 10 (2022), 100114.
[65] B.R. Lane, A.J. Stephenson, C. Magi-Galluzzi, M.M. Lakin, E.A. Klein, Urology 72 (2008) 1240–1245.
[66] A.B. Araujo, J.M. Dixon, E.A. Suarez, M.H. Murad, L.T. Guey, G.A. Wittert, J. Clin. Endocrinol. Metab. 96 (2011) 3007–3019.
[67] C.J. Houtman, S.S. Sterk, M.P.M. van de Heijning, A. Brouwer, R.W. Stephany, B. van der Burg, E. Sonneveld, Anal. Chim. Acta. 637 (2009) 247–258.
[68] A. Yarman, F.W. Scheller, Sensors 20 (2020) 2677.